Graphical Abstract

To create your abstract, type over the instructions in the template box below.
Fonts or abstract dimensions should not be changed or altered.

Leave this area blank for abstract info.

A novel 10-membered macrocyclic lactone from the mangrove-derived endophytic fungus *Annulohypoxylon* sp.

Yang Liu[a,b], Tibor Kurtán[c], Attila Mándi[c], Horst Weber[d], Changyun Wang[b], Rudolf Hartmann[e], Wenhan Lin[f], Georgios Daletos[a*], Peter Proksch[a*]

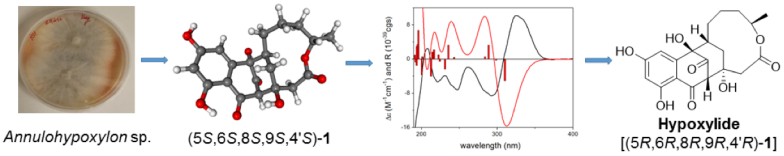

Tetrahedron Letters
journal homepage: www.elsevier.com

A novel 10-membered macrocyclic lactone from the mangrove-derived endophytic fungus *Annulohypoxylon* sp.

Yang Liu[a,b], Tibor Kurtán[c], Attila Mándi[c], Horst Weber[d], Changyun Wang[b], Rudolf Hartmann[e], Wenhan Lin[f], Georgios Daletos[a*], Peter Proksch[a*]

[a] *Institute of Pharmaceutical Biology, Heinrich-Heine-University, Universitaetsstrasse 1, D-40225 Duesseldorf, Germany.*
[b] *Key Laboratory of Marine Drugs, The Ministry of Education of China, School of Medicine and Pharmacy, Ocean University of China, Qingdao 266003, P. R. China*
[c] *Department of Organic Chemistry, University of Debrecen, P. O. B. 400, 4002 Debrecen, Hungary*
[d] *Institute of Pharmaceutical and Medicinal Chemistry, Heinrich-Heine-University, Universitaetsstrasse 1, D-40225 Duesseldorf, Germany*
[e] *Institute of Complex Systems: Strukturbiochemie, Forschungszentrum Juelich, Wilhelm-Johnen-Straße, 52428 Juelich, Germany*
[f] *State Key Laboratory of Natural and Biomimetic Drugs, Beijing University, Beijing 100191, P. R. China*

ARTICLE INFO

Article history:
Received
Received in revised form
Accepted
Available online

Keywords:
macrolactone
hypoxylide
Annulohypoxylon sp
Mangrove
endophytic fungus

ABSTRACT

A novel 10-membered macrolactone, hypoxylide (**1**), was isolated from the endophytic fungus *Annulohypoxylon* sp. that was obtained from the Mangrove plant *Rhizophora racemosa*. The structure and absolute configuration of **1** was unambiguously elucidated by comprehensive 1D and 2D NMR, as well as by HRESIMS and ECD spectroscopic analyses. Hypoxylide (**1**) features an unprecedented polyketide skeleton comprised of a trihydroxynaphthalene-dione moiety fused to a decalactone ring. A plausible biosynthetic pathway of this novel metabolite is proposed.

Mangrove endophytic fungi continue to attract attention as prolific sources of structurally unprecedented bioactive natural products.[1] It has been hypothesized that these endophytes have developed unique metabolic mechanisms as a response to various stress factors in Mangrove habitats, such as high salinity and intertidal zone alterations.[2,3] Indeed, our previous work on the Mangrove endophytic fungus *Phomopsis longicolla*, afforded the tetrahydroxanthone derivative phomoxanthone A, which showed selective pro-apoptotic activity toward several cancer cell lines, including cisplatin resistant ones, parallel to potent immunostimulatory capacity on murine T cells, NK cells, and macrophages.[4,5]

During our ongoing search for structurally unique secondary metabolites from Mangrove endophytic fungi,[6,7,8] the fungus *Annulohypoxylon* sp. which was obtained from the Mangrove plant *Rhizophora racemosa*, yielded several new daldinone derivatives.[9] As a continuation of this work, a novel macrolide, hypoxylide (**1**), possessing an unprecedented trihydroxynaphthalene-dione moiety fused to a decalactone ring is now reported (Figure 1).

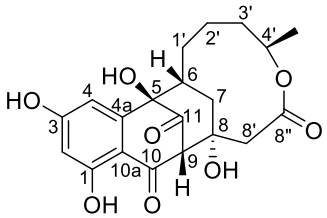

Hypoxylide (**1**)

Figure 1. Structure of compound **1**

Hypoxylide (**1**) was obtained as a light yellowish, amorphous solid. Its molecular formula was established as $C_{20}H_{22}O_8$ on the basis of the prominent ion peak observed at m/z 391.1389 $[M + H]^+$ in the HRESIMS spectrum, accounting for 13 degrees of unsaturation. The ^{1}H NMR spectrum of **1**, measured in MeOH-d_4, revealed representative signals of five sets of methylene groups resonating at δ_H 2.68/2.51 (H_2-8'), 1.95/1.31 (H_2-2'), 1.86/1.10 (H_2-1'), 1.81/1.55 (H_2-3'), and 1.64/1.21 (H_2-7), one aliphatic proton at δ_H 2.61 (H-6), one methyl group at δ_H 1.24 (4'-CH_3), one oxymethine proton at δ_H 4.70 (H-4'), and two *meta*-coupled aromatic protons at δ_H 6.27 (J = 2.4 Hz; H-2) and 6.61 (J = 2.4 Hz; H-4). The ^{13}C NMR spectrum of **1** showed 20

∗ Corresponding authors.
E-mail: georgios.daletos@uni-duesseldorf.de (G. Daletos); proksch@uni-duesseldorf.de (P. Proksch)

resonances attributable to two keto groups at δ_c 203.6 (C-11) and 195.5 (C-10), one ester group at δ_c 169.7 (C-8"), one benzene ring (δ_c 165.5, 164.5, 144.9, 112.0, 106.7, and 101.7; C-10a – C-4a), and 11 aliphatic sp^3 carbons (Supporting information Table S1). Detailed analysis of the COSY and HSQC NMR spectra revealed a long continuous spin system starting from the methylene group CH_2-7 and sequentially extending until the methyl group 4'-CH_3 (Figure 2). This spin system was confirmed by HMBC correlations from H_2-7 to C-6 and C-1', from H_2-1' to C-6, C-2', and C-3', from H_2-3' to C-2', C-4', and 4'-CH_3, as well as from 4'-CH_3 to C-3' and C-4'. In addition, the HMBC correlations from the methylene group H_2-8' to C-8, C-7, and C-8", and from H-4' to C-8" corroborated the existence of a 10-membered macrocyclic ring in **1** (Figure 2). The remaining HMBC correlations from H-2 to C-10a, C-1, C-3 and C-4, as well as from H-4 to C-10a, C-2, and C-3 further established the presence of a benzene ring (C-10a – C-4a).

Further NMR analysis of **1**, using DMSO-d_6 as solvent, afforded key HMBC correlations from 3-OH (δ_H 11.01) to C-2 and C-4, as well as from a chelated hydroxy group (δ_H 12.48, 1-OH) to C-10a, C-1, and C-2, thus assigning the location of two OH groups in the benzene ring at C-3 and C-1, respectively. Additional HMBC correlations from H-9 to C-11 and C-5, as well as from 5-OH to C-4a, C-5, and C-11 suggested the remaining keto group being located at C-11, thus indicating a 1,3-naphthalene-dione moiety in the structure of 1. Finally, the connection of this substructure with the lactone ring was established based on the HMBC correlations from 5-OH to C-6, from H-9 to C-8, C-7, and C-8', from 8-OH to C-7, C-8, C-9, and C-8', as well as from H_2-7 to C-5 and C-9 (Figure 2).

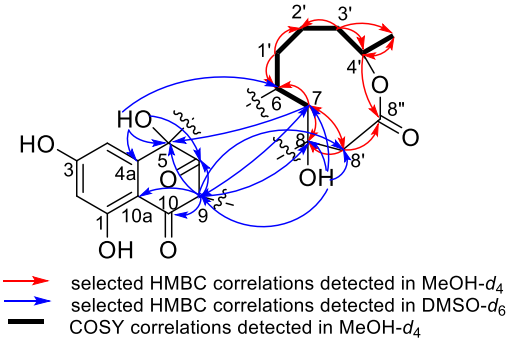

Figure 2. Selected HMBC and COSY correlations of **1**

Table 1. ^{1}H (600 MHz) and ^{13}C (150 MHz) NMR data of **1** (MeOH-d_4 and DMSO-d_6, δ in ppm)

	1 (in MeOH-d_4)		**1** (in DMSO-d_6)	
Position	δ_C	δ_H, mult. (*J* in Hz)	δ_C	δ_H, mult. (*J* in Hz)
1	164.5		163.7	
2	101.7	6.27, d (2.4)	101.7	6.25, d (2.3)
3	165.5		165.2	
4	106.7	6.61, d (2.4)	106.9	6.54, d (2.3)
4a	144.9		145.4	
5	80.3		80.2	
6	40.1	2.61, ddt (12.8, 12.0, 3.0)	39.5	2.47 (overlapping)
7	34.4	a: 1.64, dd (15.0, 12.0) b: 1.21, dd (15.0, 1.1)	34.6	a: 1.44, br d (14.2) b: 1.06, br t (14.2)
8	74.7		75.2	
9	74.6	3.31 (overlapping)	74.8	3.46, d (1.0)
10	195.5		195.6	
10a	112.0		111.7	
11	203.6		203.8	
1'	25.3	a: 1.10, ddt (13.4, 12.8, 3.5) b: 1.86, tdd (13.4, 4.6, 3.0)	25.1	a: 0.93, br t (12.8) b: 1.71, m
2'	23.7	a: 1.95, dddd (14.8, 13.4, 10.5, 3.5) b: 1.31, dddd (14.8, 9.6, 4.6, 3.5)	23.5	a: 1.83, m b: 1.18, m
3'	34.5	a: 1.81, dd (15.6, 10.5) b: 1.55, dt (15.6, 9.6)	34.1	a: 1.73, m b: 1.45, m
4'	75.7	4.70, dq (9.6, 6.2)	74.9	4.58, dd (9.9, 6.3)
4'-CH_3	20.7	1.24, d (6.2)	21.7	1.18, d (6.3)
8'	44.8	a: 2.68, d (12.8) b: 2.51, dd (12.8, 3.0)	44.7	a: 2.54, dd (12.8, 3.2) b: 2.45, dd (12.8, 2.6)
8"	169.7		168.9	
1-OH				12.48, s
3-OH				11.01, s
5-OH				6.11, s
8-OH				5.82, br s

The relative configuration of **1** was deduced by analysis of the coupling constants and the ROESY spectrum. Accordingly, key correlations of H-9 with H-8'a and H-8'b, as well as of H-1'b with both H-6 and 5-OH suggested the co-facial orientation of the respective protons. Consequently, 8-OH was oriented on the opposite side based on its correlations with both H-7a and H-7b, suggesting a chair conformation for the cyclohexanone ring. The axial orientation of H-6 was corroborated by its ROESY correlation with H-3'b, as well as by the large vicinal coupling constants with H-7a and H-1'a ($^3J_{H\text{-}6,\ H\text{-}7a}$ = 12.0 Hz and $^3J_{H\text{-}6,\ H\text{-}1'a}$ = 12.8 Hz, respectively). Finally, the ROESY cross-peaks of 4'-CH_3 with H-3'a and of H-4' with H-7b indicated the equatorial orientation of 4'-CH_3 in the lactone ring, which is in agreement with the large coupling constant (9.6 Hz) between H-4' and H-3'b (Table S1). Hence, the relative configuration (5*S**,6*S**,8*S**,9*S**,4'*S**) was deduced for **1** as shown in Figure 3.

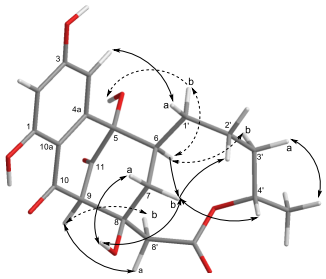

Figure 3. ROESY correlations of the arbitrarily chosen enantiomer (5*S*, 6*S*, 8*S*, 9*S*, 4'*S*)-**1**

For the determination of the absolute configuration of **1**, the solution TDDFT-ECD approach was utilized.[10,11] The initial Merck Molecular Force Field (MMFF) conformational search of the arbitrarily chosen (5*S*,6*S*,8*S*,9*S*,4'*S*) enantiomer resulted in 9 conformers in a 21 kJ/mol energy window indicating low flexibility of the molecule. Reoptimization of these conformers at the B3LYP/6-31G(d) *in vacuo* and the B97D/TZVP[12,13] PCM/MeCN levels each yielded 6 low-energy conformers over 1% Boltzmann population differing only in the orientations of the 3-OH and the 8-OH groups (Figure 4). The interatomic distances and dihedral angles of the computed conformers were in agreement with the observed ROESY correlations and $^{3}J_{H,H}$ data confirming the relative configuration. The computed ECD spectra of the individual conformers of (5*S*,6*S*,8*S*,9*S*,4'*S*)-1 were rather similar and the Boltzmann-weighted average ECD spectrum gave a nice mirror-image overall agreement with the experimental ECD spectrum (Figure 5) allowing unambiguous elucidation of the absolute configuration of **1** as (5*R*,6*R*,8*R*,9*R*,4'*R*).

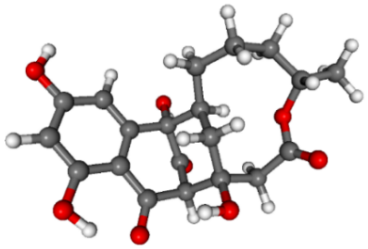

Figure 4. Six overlapped low-energy (> 1%) solution conformers of (5*S*,6*S*,8*S*,9*S*,4'*S*)-**1** with Boltzmann populations of 20.3%, 20.3%, 19.3%, 19.2%, 10.1% and 9.7% indicating that they differ only in the orientation of two OH protons. Level of optimization: B97D/TZVP PCM/MeCN.

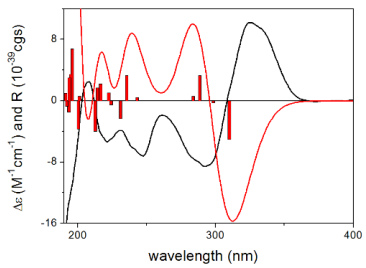

Figure 5. Experimental ECD spectrum of **1** in MeCN (black curve) compared with the Boltzmann-weighted BH&HLYP/TZVP PCM/MeCN ECD spectrum of (5*S*,6*S*,8*S*,9*S*,4'*S*)-**1** (red curve) computed for the six low-energy (> 1%) B97D/TZVP PCM/MeCN conformers. Bars represent the rotational strengths of the lowest-energy conformer.

Since for similar fused ten-membered ring systems there are examples for both *cis* and *trans* annulations,[14,15] a TDDFT-ECD study was also performed on the C-8 epimer having *cis* ring annulations of the ten-membered and (5*S*,6*S*,8*S*,9*S*,4'*S*) absolute configuration to confirm our assignment of relative configuration and exclude the *cis* annulated stereoisomer. MMFF conformational search performed on the arbitrarily chosen (5*S*,6*S*,8*R*,9*S*,4'*S*) enantiomer resulted in 38 conformers in a 21 kJ/mol energy window indicating higher flexibility of the C-8 epimer. Reoptimization of these conformers at the above mentioned DFT levels yielded 14 (supporting information Figure S14) and 1 low-energy conformers over 2% Boltzmann population (Figure 6), respectively. The geometry of the computed conformers contradicted the observed ROESY correlations.

ECD spectra computed for both sets of conformers gave mirror-image agreement for the two high-wavelength transitions but in the range of 205-260 nm region the computed and experimental transitions did not match (Figure 7). Thus, TDDFT-ECD calculations of the (5*S*,6*S*,8*R*,9*S*,4'*S*) stereoisomer could also exclude this possibility, and verified the above (5*R*,6*R*,8*R*,9*R*,4'*R*) absolute configuration for **1**.

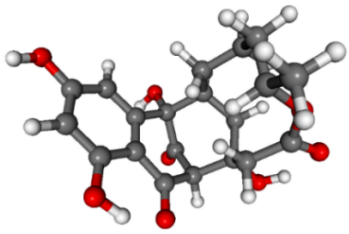

Figure 6. B97D/TZVP PCM/MeCN optimized single low-energy (> 2%) conformer of (5S,6S,8R,9S,4'S)-**1** with a Boltzmann population of 91.6%.

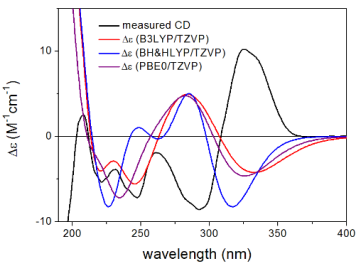

Figure 7. Experimental ECD spectrum of **1** in MeCN (black curve) compared with the Boltzmann-weighted PCM/MeCN ECD spectra of (5S,6S,8R,9S,4'S)-1 computed at various levels (red, blue and purple lines) for the single low-energy (> 1%) B97D/TZVP PCM/MeCN conformer.

A plausible biosynthetic pathway of **1** includes the condensation of an acetyl-CoA starter unit and four malonyl-CoA extender units to generate a pentaketide. The latter would then undergo cyclization and aromatization reactions to form 1,3,6,8-tetrahydroxynaphthalene (4THN), which is in equilibrium with 6,8-dihydroxy-1,3(2*H*,4*H*)-naphthalenedione[16,17], both compounds being closely related to 3,4-dihydro-3,4,6,8-tetrahydroxy-l(2*H*)-naphthalenone and (*R*)-scytalone, which have been previously isolated from the same *Annulohypoxylon* sp.

strain.[9] Alternatively, the initial pentaketide could undergo regiospecific reduction, dehydration, and lactonization to yield the 10-membered macrolide diplodialide A, a known metabolite from the fungus *Diplodia pinea*.[18,19] Finally, tandem Michael-aldol addition of these subunits and subsequent hydroxylation at position 5 would result in the formation of **1** (Figure 8).

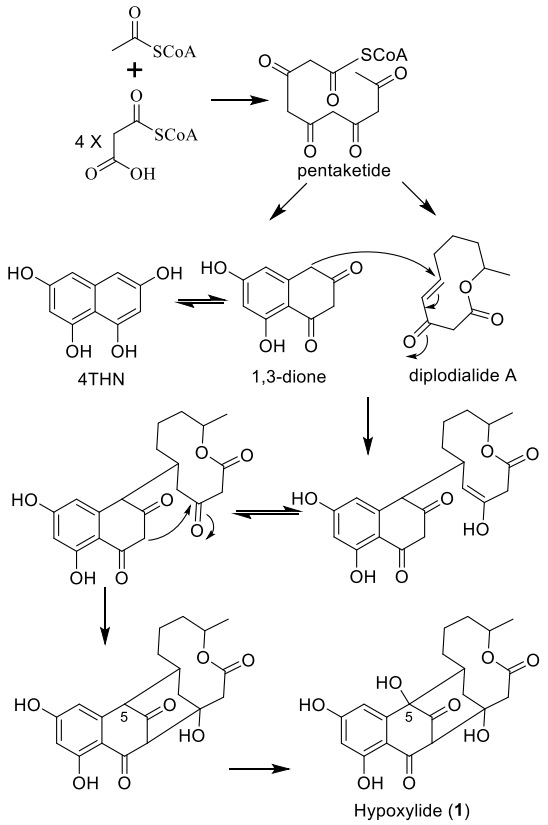

Figure 8. Proposed biosynthesis of **1**.

Hypoxylide (**1**) was screened for cytotoxicity against mouse lymphoma (L5178Y), human leukemia (Jurkat J16), and human lymphoma (Ramos) cell lines using the MTT assay, as well as for its antibacterial activity against *Staphylococcus aureus* ATCC 25923, *Acinetobacter baumannii* ATCC BAA747, and *Mycobacterium tuberculosis*. However, compound 1 did not show any detectable activity when assayed at an initial dose of 10 μM.

In conclusion, a new 10-membered macrolactone, hypoxylide (**1**), was isolated and characterized from a Mangrove-derived endophytic fungus belonging to *Annulohypoxylon* genus. The structure and absolute configuration of **1** were unambiguously established by comprehensive 1D and 2D NMR, along with HRESIMS and ECD spectroscopic analysis. Compound **1** features a unique polyketide scaffold bearing a trihydroxynaphthalene-dione moiety fused to a decalactone ring. The latter moiety resembles that found in benzenediol lactones (BDLs) (e.g., curvularin and sonnerlactones);[20,21] however, to the best of our knowledge, the present study represents the first example of a 1,3-fused ten-membered ring system forming an unusual C-6 – C-8 coupling pattern in the structure of **1**. Notably, molecular studies have shown that BDLs are biosynthesized by two sequentially acting iterative polyketide synthases,[20,22] thus producing chimeric scaffolds, which is in accordance with the proposed biosynthetic pathway of **1** involving the linkage of two pentaketides, 6,8-dihydroxy-1,3(2*H*,4*H*)-naphthalenedione and diplodialide A. Overall, the novel structure of **1** not only expands the structural diversity of polyketide lactone scaffolds in nature, but also provides further insights into their biogenesis, thus offering an attractive target for synthetic and biosynthetic research communities alike.

Acknowledgements

Financial support by the DFG through the GRK 2158 to P. P. is gratefully acknowledged. W. H. L. wants to thank the Ministry of Science and Technology (MOST) for support. T. K. and A. M. thank the National Research, Development and Innovation Office (NKFI K 120181 and PD 121020) for financial support and the Governmental Information-Technology Development Agency (KIFÜ) for CPU time. The authors are indebted to Prof. R. Kalscheuer (Heinrich-Heine-University, Duesseldorf) for performing antibacterial assays, to Prof. W. E. G. Müller (Johannes Gutenberg University, Mainz, Germany), to Dr. B. Stork for cytotoxicity assays, to Dr. S. H. Akone (University of Douala, Cameroon) for collecting the plant, and to Prof. B. Henrich (University Clinic of the Heinrich Heine University, Germany) for the fungal identification.

References

1. Debbab, A.; Aly, A. H.; Proksch, P. *Fungal Divers.* **2013**, *61*, 1-27.
2. Xu, D. B.; Ye, W. W.; Han, Y.; Deng, Z. X.; Hong, K. *Mar. Drugs* **2014**, *12*, 2590-2613.
3. Li, J. L.; Sun, X.; Chen, L.; Guo, L. D. *Mycology* **2016**, *7*, 180-190.
4. Rönsberg, D.; Debbab, A.; Mándi, A.; Vasylyeva, V.; Böhler, P.; Stork, B.; Engelke, L.; Hamacher, A.; Sawadogo, R.; Diederich, M.; Wray, V.; Lin, W.; Kassack, M. U.; Janiak, C.; Scheu, S.; Wesselborg, S.; Kurtán, T.; Aly, A. H.; Proksch, P. *J. Org. Chem.* **2013**, *78*, 12409-12425.
5. Frank, M.; Niemann, H.; Böhler, P.; Stork, B.; Wesselborg, S.; Lin, W.; Proksch, P. *Curr. Med. Chem*. **2015**, *22*, 3523-3532.
6. Hemphill, C. F. P.; Daletos, G.; Liu, Z.; Lin, W.; Proksch, P. *Tetrahedron Lett.* **2016**, *57*, 2078-2083.
7. Moussa, M.; Ebrahim, W.; El-Neketi, M.; Mándi, A.; Kurtán, T.; Hartmann, R.; Lin, W.; Liu, Z.; Proksch, P. *Tetrahedron Lett.* **2016**, *57*, 4074-4078.
8. Liu, S.; Dai, H.; Makhloufi, G.; Heering, C.; Janiak, C.; Hartmann, R.; Mándi, A.; Kurtán, T.; Müller, W. E. G.; Kassack, M. U.; Lin, W.; Liu, Z.; Proksch, P. *J. Nat. Prod.* **2016**, *79*, 2332-2340.
9. Liu, Y.; Stuhldreier, F.; Kurtán, T.; Mándi, A.; Arumugam, S.; Lin, W.; Stork, B.; Wesselborg, S.; Weber, H.; Henrich, B.; Daletos, G.; Proksch, P. *RSC Adv.* **2017**, *7*, 53815393.
10. Pescitelli, G.; Bruhn, T. *Chirality* **2016**, *28*, 466-474.
11. Mándi, A.; Mudianta, I. W.; Kurtán, T.; Garson, M. J. *J. Nat. Prod.* **2015**, *78*, 2051–2056.
12. Grimme, S. *J. Comput. Chem.* **2006**, *27*, 1787-1799.
13. Sun, P.; Xu, D. X.; Mándi, A.; Kurtán, T.; Li, T. J.; Schulz, B.; Zhang, W. *J. Org. Chem.* **2013**, *78*, 7030-7047.
14. Roe, M. B.; Whittaker, M.; Procter, G. *Tetrahedron Lett.* **1995**, *36*, 8103-8106.
15. Uchio, Y.; Kubota, N. K.; Haino, T.; Fukazawa, Y. *B. Chem. Soc. Jpn.* **2006**, *79*, 914-920.
16. Highet, R. J.; Ekhato, I.V. *J. Org. Chem.***1988**, *53*, 2843-2844.
17. Ichinose, K.; Sugimori, M.; Itai, A.; Ebizuka, Y.; Sankawa, U. *Tetrahedron Lett.* **1990**, *31*, 5905-5908.
18. Wada, K.; Ishida, T. *J.C.S. Perkin Trans I* **1979**, *1*, 1154-1158.
19. Wakamatsu, T.; Akasaka, K.; Ban, Y. *J. Org. Chem.* **1979**, *44*, 2008-2012.
20. Bai, J.; Lu, Y.; Xu, Y.; Zhang, W.; Chen, M.; Lin, M.; Gunatilaka, A. A. L.; Xu, Y.; Molnár, I. *Org. Lett.* **2016**, *18*, 1262-1265.
21. Li, K. K.; Lu, Y. J.; Song, X. H.; She, Z. G.; Wu, X. W.; An, L. K.; Ye, C. X.; Lin, Y. C. *Bioorg. Med. Chem. Lett.* **2010**, *20*, 3326-3328.

22. Xu, Y.; Espinosa-Artiles, P.; Schubert, V.; Xu, Y. M.; Zhang, W.; Lin, M.; Gunatilaka, A. A.; Süssmuth, R.; Molnár, I. *Appl. Environ. Microbiol.* **2013**, *79*, 2038-2047.

Supplementary Material

Electronic Supplementary Information (ESI) available: General experimental procedures, fungus material, extraction and isolation, characterization data, bioassays, copies of HRESIMS, 1D and 2D NMR spectra of **1**, as well as low-energy conformers of (5*S*,6*S*,8*R*,9*S*,4'*S*)-**1** are available.